DOI: 10.1002/ejic.200900978

Synthesis of Highly Stable CdTe/CdS Quantum Dots with Biocompatibility

Ying-Fan Liu,*[a] Bing Xie,[a] Zhi-Gang Yin,[a] Shao-Ming Fang,*[a] and Jian-Bo Zhao[a]

Keywords: Cadmium / Dihydrolipoic acid / Luminescence / Quantum dots / Biocompatibility / Semiconductors

Thioglycolic acid (TGA) is a popular coating material for the preparation of aqueous quantum dots (QDs), yet dihydrolipoic acid (DHLA) has not been studied much. Here we present a detailed study on the aqueous synthesis of CdTe/CdS quantum dots with a DHLA coating. The outer CdS shell and DHLA stabilizer provide efficient confinement of electron and hole wave functions inside the nanocrystal as well as high photochemical stability. At the optimum ratios and reaction conditions, the results indicate that the DHLA-capped CdTe/CdS QDs exhibit high fluorescence quantum yields (QYs) of about 48 % over a spectral range of 551–571 nm, and the best QY is 87 %. These DHLA-capped core–shell QDs are highly biocompatible and monodisperse. In particular, they have exhibited excellent colloidal and photostability over one year of study. The synthesis of QDs by using DHLA as stabilizer is simple and environmentally friendly, and it can easily be extended to the large-scale, aqueous-phase production of QDs. At a QD dose of 120 μg/mL, TGA-stabilized CdTe QDs induce 9.5 % hemolysis, whereas DHLA-stabilized CdTe/CdS QDs induce only 3 % hemolysis. Hemolytic results indicate that DHLA-stabilized QDs are more biocompatible than TGA-capped CdTe QDs, which is especially important for QDs as biomarkers in biological detection and diagnosis.

Introduction

Luminescent semiconductor quantum dots (QDs), due to their excellent optical properties, high emission quantum yield (QY), size-dependent emission wavelength, and high photostability etc., have been rapidly developed.[1,2] As semiconductor nanocrystals (NCs) possess versatile functions, they are suitable for bioapplications such as labeling in living cells, in vivo imaging, and diagnostics.[3–7] The key parameters that determine the applicability of luminescent NCs in real situations are (i) high luminescence quantum efficiency, (ii) stability of luminescence properties under real operation conditions, (iii) biocompatibility and solubility of NCs in a biosystem. All these problems are connected with the proper passivation of dangling bonds present on the nanocrystal surface.

Up to date, many studies have been conducted to synthesize II-VI semiconductor NCs, especially aqueous semiconductor NCs for bioapplications. CdTe QDs are an important type of semiconductor NCs. On the one hand, the selection of capped reagents is an important strategy in aqueous synthesis. Attaching organic ligands to the nanocrystal surface can provide solubility to nanocrystals and, in certain cases, allow high photoluminescence (PL) quantum efficiency. The QYs of CdTe QDs can be improved by selecting appropriate ligand molecules such as thioglycolic acid (TGA), 3-mercaptopropionic acid (MPA) and optimizing the ratio of capping ligands to cadmium.[8–16] On the other hand, high-quality core–shell quantum dots can be prepared by epitaxial growth of a shell on the surface of the core, which is an effective approach to eliminate the surface dangling bonds and improve the spectral properties of NCs.[17–19] However, studies have mostly focused on the improvement of the spectral properties of QDs; the stability and biocompatibility of QDs have received less attention.

In recent years, an increasing number of papers examined the interactions between cells and nanoparticles.[20] Determination of hemolytic properties is one of the most common tests in studies of nanoparticle interaction with blood components.[21–23] Hemolytic activity is highly dependent upon nanostructured material surface environments (e.g. morphology, charge, porosity) as well as material composition.[24–26] In our studies, hemolysis assays were used to explore the differential biocompatibility of CdTe-TGA and CdTe/CdS-DHLA QDs with red blood cells of rabbits.

In this article, we present a novel strategy of synthesis of highly stable CdTe/CdS quantum dots in aqueous solution by using the DHLA ligand as stabilizer. With CdTe QDs as core template, DHLA-capped CdTe/CdS QDs were synthesized in aqueous solution by simple refluxing at 100 °C. The DHLA-capped CdTe/CdS QDs exhibit high fluorescence QYs of about 48 % over a spectral range of 551–571 nm, and the best QY is 87 % without any post-preparative treatment. When hemolytic studies are used to compare TGA and DHLA as stabilizer, the results indicate that DHLA is more environmentally friendly in aqueous synthesis and highly biocompatible in using the QDs as biological probes.

[a] College of Material and Chemical Engineering, Zhengzhou University of Light Industry, Henan Provincial Key Laboratory of Surface and Interface Science,
Zhengzhou 450002, P. R. China
E-mail: yfliu@zzuli.edu.cn
mingfang@zzuli.edu.cn

Supporting information for this article is available on the WWW under http://dx.doi.org/10.1002/ejic.200900978.

This approach can easily be extended to the large-scale, aqueous-phase production of core–shell QDs. The CdTe/CdS QD system is expected to find wide applications in biological detection and diagnostics.

Results and Discussion

The Synthesis and Optical Properties of CdTe/CdS QDs

Previous research has focused on the synthesis of highly luminescent thiol-stabilized CdTe, but the stability of the QDs has been rarely reported. In this study, we selected DHLA molecules as capping reagents to synthesize CdTe/CdS QDs in the aqueous phase. The molecular structure of DHLA is shown in Scheme 1. Although highly luminescent CdTe/CdS QDs can be synthesized by illumination for 10–25 d or by microwave irradiation in the aqueous phase,[17–19] these methods have the disadvantages of high costs or long reaction times. Thus, to overcome this deficiency, we designed a simple route to quickly synthesize CdTe/CdS with high QYs in aqueous solution. Firstly, the core CdTe QDs are prepared by refluxing a mixture of solutions of Cd^{2+}, NaHTe, and TGA (Cd^{2+}/Te/TGA = 4:1:8) at ambient conditions at 100 °C. The as-prepared TGA-capped CdTe QDs are precipitated with 2-propanol, and the supernatant is decanted to remove the excess Cd^{2+} and TGA. The CdTe QDs obtained by precipitation are redissolved in alkaline solution containing Cd^{2+} and DHLA, so that excess Cd^{2+} ions and DHLA occupy the vacancies on the surface of the CdTe QDs. Then, thioacetamide (TAA) is added to the DHLA-capped CdTe QD solution. After refluxing for ten minutes to several hours at 100 °C, various sizes of high-quality core–shell CdTe/CdS QDs can be obtained. Figure 1 presents typical evolutions of both absorption and photoluminescence spectra of the TGA-stabilized CdTe core and the DHLA-capped CdTe/CdS core–shell QDs prepared in aqueous solution. The size of the original core CdTe QDs is 2.2 nm, which is calculated from the electronic transition at 504 nm (Figure 1A) of the CdTe QDs.[27] The PL emission peak of the core CdTe QDs is at 548 nm with a QY of 52% (Figure 1B). When TAA is added to the aqueous solution of CdTe QDs, while refluxing at 100 °C, a slight redshift of the excitonic absorption and PL emission of the solution is observed. As shown in Figure 1A, the excitonic absorption peaks of the QD system shift to the red from 503 nm to 507 nm and then to 525 nm after refluxing for 10 min to 20 h. These excitonic absorption peaks of the QD solution are attributed to the 1s–1s electronic transition of the corresponding QDs. Under reflux, the redshift of the excitonic absorption wavelength of the QDs implies that the size of the QDs increases, the maximum increment in their size is calculated to be 0.3 nm: the QDs grow from 2.2 nm (core) to 2.5 nm. As the core CdTe nanoparticles rich in cadmium ions and S^{2-} released from TAA are in the reaction solution and the excitonic absorption of single CdS clusters is not observed, the increase in the size of the QDs indicates that a CdS shell may form on the surface of the CdTe core QDs, that is, core–shell CdTe/CdS QDs form. With ongoing reflux, a sequence of redshifts of the corresponding PL emission wavelengths and changes of QYs of the QD solutions (Figure 1B) further provide evidence for the formation of core–shell CdTe/CdS QDs. The photoluminescence emission wavelengths and QYs of the CdTe/CdS QDs are: 551 nm 60%, 552 nm 64%, 554 nm 67%, 556 nm 71%, 557 nm 77%, 558 nm 81%, 564 nm 87%, 567 nm 63%, and 571 nm 48%. After refluxing for 7 h, the emission wavelength of the QDs changes from 548 nm to 564 nm, the photoluminescence intensity reaches a plateau, and the PL QY is 87%. Compared with the PL QY of the core CdTe crude solution, the PL QY of the new core–shell QDs is greatly enhanced: it is about 1.6 times after refluxing for 7 h. The emission of CdTe nanocrystals capped with other thiols such as thioglycolic acid (TGA) and mercaptoprop-

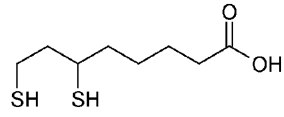

Scheme 1. The molecular structure of DHLA.

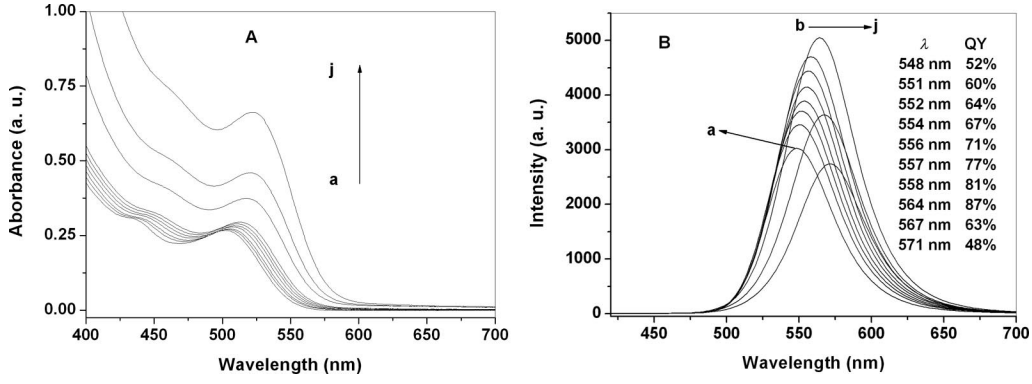

Figure 1. Typical temporal evolution of the absorption (A) and corresponding emission (B) spectra of TGA-CdTe core and core–shell CdTe/CdS QDs. Curve (a) represents the absorption (A) and corresponding emission (B) spectra of CdTe core QDs. Curves (b), (c), (d), (e), (f), (g), (h), (i), and (j) represent the absorption (A) and corresponding emission (B) spectra of CdTe/CdS QDs obtained after refluxing for 10, 20 min, 0.5, 1, 2, 4, 7, 10, and 20 h, respectively; the excitation wavelength is 400 nm.

ionic acid (MPA) can be tuned from green to near-IR wavelengths.[16] Here, when green-emitting particles (CdTe, 548 nm) were used as core template and DHLA as capping reagent, only green-yellow emitting particles were obtained. A typical characteristic of the present capping is that the bidentate dihydrolipoic acid (Scheme 1) can make a simultaneous capping attachment to two surface sites on the CdS overcoating shell, theoretically resulting in more stable cap/shell interactions. Differences in surface properties for dots capped with lipoic acid relative to those capped with monothiol may significantly alter the growth of the QDs.

Influence of the TAA/Cd^{2+} Ratio

The success of our approach strongly depended on optimal experimental conditions. In order to obtain high-quality CdTe/CdS core–shell QDs, the influence of the molar ratio of TAA/Cd^{2+} was investigated. For this experiment, we varied the amount of TAA from 0 to 0.72 mmol while keeping the other experimental variables such as the amount of DHLA and CdTe core, the pH value, the reaction time (7 h), and the reaction temperature fixed. Figure 2 shows the strong influence of the TAA/$CdCl_2$ ratio on the PL intensity of the as-prepared CdTe/CdS QDs. The PL intensity increases steadily when the QD system is refluxed for 7 h and the molar ratio of TAA to $CdCl_2$ increases from 0 to 0.36:1, while the PL intensity decreases slightly when the ratio is higher than 0.36:1. The reason was ascribed to the increase in the CdS growth rate with the increase in the TAA/Cd ratio, but a greater amount of TAA is not beneficial for CdS shell growth.

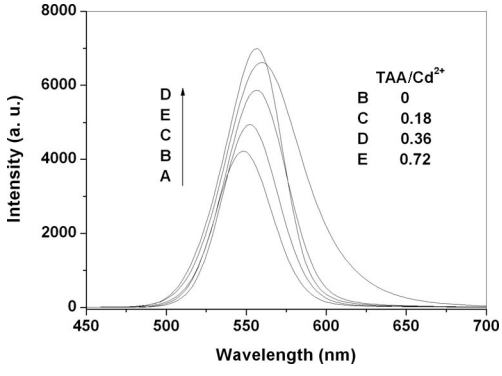

Figure 2. PL spectra of DHLA-stabilized CdTe (A, B) and CdTe/CdS (C, D, E) QDs. Curve (A) shows the PL spectrum of the CdTe core QDs, and curves (B)–(E) are PL spectra of the QDs obtained after refluxing for 7 h at various precursor TAA/Cd^{2+} molar ratios.

TEM, XRD, and XPS Characterization

In order to confirm the formation of CdS shells on CdTe cores in aqueous solution, X-ray photoelectron spectroscopy (XPS) and powder XRD measurements were made. At the same time, aqueous CdTe/CdS NCs were characterized by transmission electron microscopy (TEM). A full survey scan and Cd, Te, S photoelectron spectra of the CdTe and CdTe/CdS NCs are displayed in Figure 3. In addition to the Cd3d core levels, the spectra are dominated by the C1s and O1s signals stemming from the capping agent. XPS spectra in Figure 3 shown that there exist Cd3d, Te3d, and S2p levels for CdTe and CdTe/CdS QDs. It is evident that, compared with the CdTe core, there is a higher content of sulfur and a lower content of tellurium on the CdTe/CdS surfaces (shown in Figure S1). These XPS data provide the direct evidence for the formation of CdTe/CdS QDs.

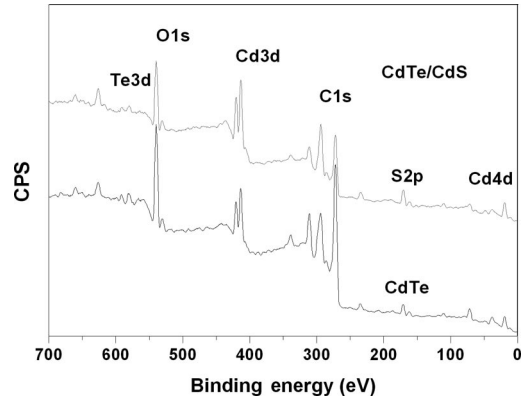

Figure 3. XPS spectra of CdTe and CdTe/CdS NCs.

The powder XRD patterns for the CdTe and CdTe/CdS NCs are depicted in Figure 4. The XRD patterns were obtained from CdTe and CdTe/CdS powders, which were precipitated from aqueous solution with an excess of 2-propanol. The precipitate was isolated by centrifugation and dried at vacuum. The characteristic zinc blende planes of 111, 220, and 311 located at 24.47°, 40.73°, and 47.48° for CdTe and at 26.31°, 42.90°, and 49.78° for CdTe/CdS in the 2θ range of 10 to 60° are observed. The position of the XRD peaks of CdTe cores matched well with those of bulk CdTe cubic structures (JCPDS NO. 15–0770). After growth of the CdS shell on the CdTe core, the peak position shifted

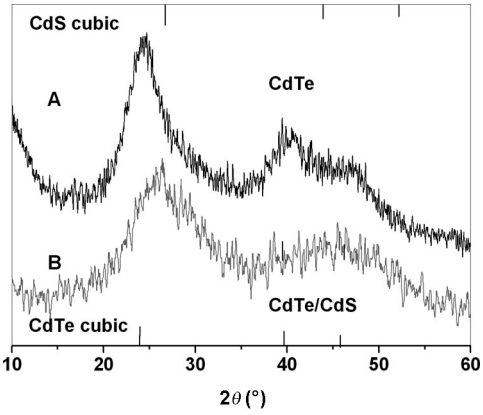

Figure 4. XRD patterns of TGA-capped CdTe (top) and DHLA-capped CdTe/CdS (bottom) NCs. The standard diffraction lines of cubic CdTe and cubic CdS are also shown for comparison.

to higher angles towards the positions of bulk CdS cubic structure peaks (JCPDS NO.10–454), which proves the formation of CdTe/CdS. The TEM image in Figure 5 shows that the CdTe/CdS NCs possess a well-dispersed crystalline structure and have a diameter of about 2.5 nm, as calculated from the absorption spectrum.[27]

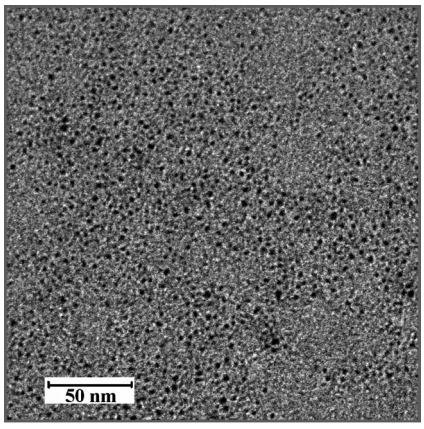

Figure 5. TEM image of CdTe/CdS samples taken from the reaction solution after refluxing for 7 h.

Oxidation by H_2O_2

The as-prepared DHLA-capped core–shell QDs have exhibited excellent colloidal and photostability over one year of study. In order to further study the stability of the QDs, we investigated the tolerance of TGA-capped CdTe and DHLA-capped CdTe/CdS QDs against chemical oxidation by H_2O_2. In the experiment, 0.015 mL of a 3% H_2O_2 solution was added to 2.0 mL of CdTe or CdTe/CdS QDs with an identical optical density of 0.15 with stirring under ambient conditions at room temperature. The PL spectra were measured after different intervals of etching time. The time dependence of the normalized PL intensities of the two samples is shown in Figure 6. As the H_2O_2 was added to the two QDs, there was an evident decrease in the PL intensity in both samples, and after that the decrease was relaxed. After 24 min of etching time, there was only 8% luminescence in the CdTe QDs, while 42% of the PL intensity of the CdTe/CdS QDs was still there, which indicated clearly that the PL tolerance of the CdTe/CdS QDs against etching with H_2O_2 is stronger than that of the CdTe QDs. Therefore, using DHLA as stabilizer, we have synthesized not only highly luminescent QDs, but also highly stable QDs in aqueous solution.

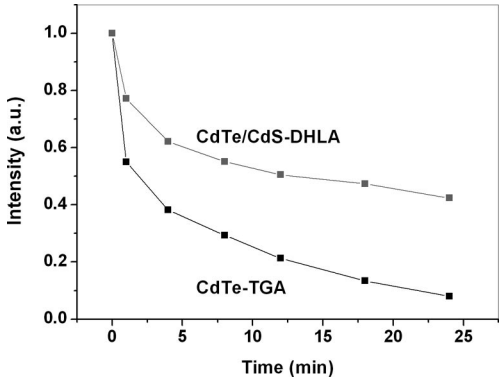

Figure 6. Time dependence of the normalized PL intensities of CdTe and CdTe/CdS core–shell samples against H_2O_2 etching time. The excitation wavelength is 400 nm.

Hemolysis Assay

Erythrocyte interaction with QDs is particularly important in the use of QDs for in vivo applications. Hemolysis is one of indicators of interaction and incompatibility of QDs with red blood cells.[28] Figure 7 and Figure S2 show the results for the determination of the hemolytic properties of CdTe-TGA and CdTe/CdS-DHLA QDs. In this commonly used protocol, the QDs were incubated in purified erythrocytes, the blood was centrifuged to remove undamaged erythrocytes, and the percent hemolysis was determined by colorimetric detection of hemoglobin in the supernatant. As shown in Figure 7, with prolonged incubation of QDs and erythrocytes (3 h at 37 °C), the hemolysis rates of CdTe-TGA and CdTe/CdS-DHLA QDs increased from 3.0% to 18.2% (CdTe) and from 0.8% to 6.7% (CdTe/CdS). The results show that higher hemolysis occurred for the QDs with higher doses. The dose-dependent hemolysis is better fitted by the linear functions $y = 0.0936x - 1.53$ ($R = 0.991$) for CdTe QDs and $y = 0.03772x - 0.91$ ($R = 0.997$) for CdTe/CdS QDs. The slope of the plot for CdTe/CdS QDs is less than that of the CdTe QD plot. For the same conditions such as incubation time, incubation temperature (37 °C), and QD dose, the percent hemolysis of the CdTe/CdS QDs is evidently less than that of CdTe QDs. For example, when the final concentration of QDs is 120 μg/mL, CdTe QDs induce over 9% hemolysis when in contact with erythrocytes for 3 h, whereas the

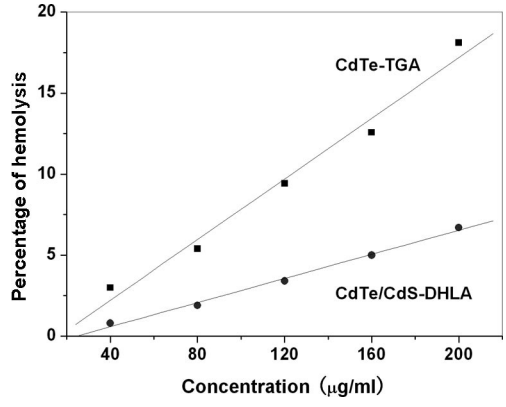

Figure 7. Concentration dependences of hemolysis induced by CdTe-TGA (top) and CdTe/CdS-DHLA QDs (bottom). The incubation time of QDs with erythrocytes is 3 h at 37 °C, and the final concentrations of QDs are 40, 80, 120, 160, and 200 μg/mL, respectively (from left to right).

hemolysis induced by CdTe/CdS QDs is lower than 5%. These studies show that CdTe/CdS-DHLA QDs are more biocompatible relative to CdTe-TGA QDs.

Conclusion

We have developed the synthesis of a novel type of luminescent semiconductor nanocrystals consisting of a CdTe core and a CdS outer shell. The comparison of DHLA-capped CdTe/CdS QDs with CdTe particles shows that introducing a CdS wetting layer and DHLA stabilizer results in (i) a significant improvement of the luminescence of the nanocrystals; (ii) more stable luminescence upon CdS shell growth, and (iii) better biocompatibility by using DHLA as capping reagent.

Experimental Section

Chemicals: Thioctic acid (TA, 98%), thioglycolic acid (TGA, 95%), $NaBH_4$ (96%), and tellurium powder (99.9%) were obtained from Sigma, Inc. Thioacetamide (TAA, 99%) and $CdCl_2$ were obtained from Shanghai Chemical Reagents Company. Ultrapure water with a conductivity of 18.2 MΩ/cm was used in all syntheses.

Synthesis of DHLA: DHLA was synthesized by reduction of TA according to published procedures.[29,30] $NaBH_4$ (1.60×10^{-3} mol) was added by small portions to an alkaline aqueous solution of TA (1.50×10^{-3} mol in 10 mL of 0.25 M NaOH solution). The vigorously stirred mixture was cooled and kept at 5 °C. After 2 h, the colorless solution was acidified to pH 1. DHLA was extracted three times from the crude product with diethyl ether (20 mL). The organic phase was washed with Ultrapure water and dried with anhydrous magnesium sulfate. The solvent was removed under reduced pressure at room temperature. The purification by chromatography (DMSO/MeOH, 9:1) provided pure DHLA (light yellow liquid). Yield: 90%.

Synthesis of CdTe QDs: TGA-capped CdTe NCs were directly synthesized by a technique that used cadmium chloride and hydrogen telluride gas.[31] The concentration of Cd^{2+} was set as 4×10^{-3} M, and the molar ratio of Cd/Te/TGA was 1:0.25:2 in our experiments. Typically, under a robust flow of nitrogen, $CdCl_2 \cdot 2.5H_2O$ (91.3 mg, 0.4 mmol) was dissolved in Milli-Q water (100 mL), and TGA (0.8 mmol, 61.7 μL) was added. Dropwise addition of NaOH (0.5 M) was then used to adjust the pH to 10 under vigorous stirring.

The method for preparation of excess NaHTe, which is described elsewhere,[32] was modified. Briefly, NaHTe solution was prepared by mixing $NaBH_4$ and tellurium powder in the presence of water and ethanol (3:1). The solution was deaerated with N_2 and heated at 50 °C for 30 min. N_2-saturated sulfuric acid (4 mL, 0.5 M) was added dropwise to the excess NaHTe solution to generate H_2Te, which was passed through NaOH solution (0.5 mL, 0.2 M) to produce NaHTe solution (0.1 mmol) under a slow flow of nitrogen. Then, NaHTe was added to the cadmium and thiol solution. The resulting solution mixture was heated to 100 °C under ambient conditions and refluxed for 30 min. Then, 2-propanol was added to the as-prepared CdTe QD colloid solution. CdTe QDs were precipitated from the solution and collected by centrifugation. Finally, the obtained CdTe QDs were dried at room temperature under vacuum.

Synthesis of CdTe/CdS QDs: A typical synthesis of CdTe/CdS core–shell NCs was performed as follows: An as-prepared CdTe core sample (40 mg) was dissolved in a solution (50 mL) containing $CdCl_2$ (2.0 mmol/L) and DHLA (5.0 mmol/L) at pH 9.5. The resulting solution mixture was heated to 100 °C under ambient conditions, and then TAA (0.36 mmol) was added. The solution was refluxed for different periods of time in order to control the size of the core–shell QDs. This method is simple and the quantities can be easily scaled. Aliquots of the reaction solution were removed at regular intervals for UV absorption and PL experiments. Samples were precipitated with 2-propanol and dried in a vacuum oven for XRD and XPS characterization. The TEM sample was prepared by dropping the aqueous CdTe/CdS solution onto carbon-coated copper grids and evaporating the excess solvent.

Hemolysis Assay: This method was modified from a published procedure.[33] Blood was drawn from a rabbit into an evacuated siliconized glass tube and stirred to remove fibrinogen production. The blood was diluted with an isotonic phosphate buffer solution (PBS) at pH 7.4 and centrifuged at 2000 rpm for 10 min, and the supernatant was discarded. The erythrocytes were washed until the supernatant was clear, and the packed cells were resuspended in PBS (pH 7.4) to obtain a 2% concentration of red blood cells. Two kinds of QDs, including TGA-capped CdTe and DHLA-capped CdTe/CdS QDs, were used to carry out the hemolytic assay. The QDs were precipitated with 2-propanol and redissolved in PBS for hemolytic characterization. The procedure of the hemolysis assay was as follows: the resultant erythrocyte suspension (2 mL), each of the two kinds of QDs at different final doses (0, 40, 80, 120, 160 and 200 μg/mL), and appropriate amounts of PBS (the total volume: 4 mL) were mixed and incubated together for 3 h at 37 °C in an orbital shaker. The mixtures were centrifuged at 2500 rpm for 10 min, and the supernatant liquids were removed. The degree of hemolysis was determined by measuring the absorbance of the supernatant at 540 nm and subtracting the absorbance of the QDs. Isotonic PBS and deionized water were used as negative and positive controls, respectively. The absorbance value accounted for the amount of hemoglobin release induced by QDs. The hemolysis was calculated on the basis of the average of three replicates.

$$\text{Hemolysis} = \frac{\text{OD(test)} - \text{OD(negative control)}}{\text{OD(positive control)} - \text{OD(negative control)}} \times 100$$

Characterization: UV/Vis absorption and photoluminescence (PL) spectra were measured at room temperature with a Shimadzu UV-3100 spectrophotometer and a Hitachi 7000 fluorescence spectrometer, respectively. PL spectra were taken at the excitation wavelength λ_{ex} = 400 nm and at the excitonic absorption peak for PL QYs. Estimates of the photoemission QYs were obtained by comparing the integrated emission from Rhodamine 6G in ethanol (QY = 0.95) and quinine in aqueous H_2SO_4 (0.5 M; QY = 0.55). Concentrations were adjusted such that both reference and QD samples gave optical densities of 0.05 at the excitation wavelength, and solvent refractive indexes were taken into account.[34,35] Powder XRD measurements were performed with a Philips X′Pert PRO X-ray diffractometer. High-resolution transmission electron microscopy (HRTEM) was performed with a Philips FEI Tecnai G^2 20 S-TWIN instrument.

Supporting Information (see footnote on the first page of this article): XPS spectra of CdTe/CdS-DHLA and CdTe-TGA QDs and concentration dependence of hemolysis induced by CdTe-TGA QDs, CdTe/CdS-DHLA QDs, and control reagents.

Acknowledgments

This work was supported by the National Natural Science Foundation of China (No. 20771095) and School Doctoral Foundation of Zhengzhou University of Light Industry.

[1] I. L. Medintz, H. T. Uyeda, E. R. Goldman, H. Mattoussi, *Nat. Mater.* **2005**, *4*, 435–436.
[2] X. Michalet, F. F. Pinaud, L. A. Bentolila, J. M. Tsay, S. Doose, J. J. Li, G. Sundaresan, A. M. Wu, S. S. Gambhir, S. Weiss, *Science* **2005**, *307*, 538–544.
[3] N. Tesste, V. Medvedev, M. Kazes, S. Kan, U. Banin, *Science* **2002**, *95*, 1506–1508.
[4] M. J. Bruchez, M. Moronne, P. Gin, S. Weiss, A. P. Alivisatos, *Science* **1998**, *281*, 2013–2016.
[5] H. Peng, L. Zhang, T. H. M. Kjallman, C. Soeller, J. Travas-Sejdik, *J. Am. Chem. Soc.* **2007**, *129*, 3048–3049.
[6] J. Ma, J.-Y. Chen, Y. Zhang, P.-N. Wang, J. Guo, W.-L. Yang, C.-C. Wang, *J. Phys. Chem. B* **2007**, *111*, 12012–12016.
[7] Z. Deng, Y. Zhang, J. Yue, F. Tang, Q. Wei, *J. Phys. Chem. B* **2007**, *111*, 12024–12031.
[8] M. Gao, A. L. Rogach, A. Kornowski, S. Kirstein, A. Eychmuller, H. Mohwald, H. Weller, *J. Phys. Chem. B* **1998**, *102*, 8360–8363.
[9] N. Gaponik, D. V. Talapin, A. L. Rogach, K. Hoppe, E. V. Shevchenko, A. Kornowski, A. Eychmuller, H. Weller, *J. Phys. Chem. B* **2002**, *106*, 7177–7185.
[10] A. Shavel, N. Gaponik, A. Eychmüller, *J. Phys. Chem. B* **2006**, *110*, 19280–19284.
[11] S. J. Byrne, Y. Williams, A. Davies, S. A. Corr, A. Rakovich, Y. K. Gun′ko, Y. P. Rakovich, J. F. Donegan, Y. Volkov, *Small* **2007**, *3*, 1152–1156.
[12] Q. Wang, Y. Kuo, Y. Wang, G. Shin, C. Ruengruglikit, Q. Huang, *J. Phys. Chem. B* **2006**, *110*, 16860–16866.
[13] H. Zhang, L. Wang, H. Xiong, L. Hu, B. Yang, W. Li, *Adv. Mater.* **2003**, *15*, 1712–1715.
[14] J. Guo, W. Yang, C. Wang, *J. Phys. Chem. B* **2005**, *109*, 17467–17473.
[15] H. Zhang, D. Y. Wang, B. Yang, H. Möhwald, *J. Am. Chem. Soc.* **2006**, *128*, 10171–10180.
[16] A. L. Rogach, T. Franzl, T. A. Klar, J. Feldmann, N. Gaponik, V. Lesnyak, A. Shavel, A. Eychmuller, Y. P. Rakovich, J. F. Donegan, *J. Phys. Chem. C* **2007**, *111*, 14628–14637.
[17] H. Bao, Y. Gong, Z. Li, M. Gao, *Chem. Mater.* **2004**, *16*, 3853–3859.
[18] Y. He, H.-T. Lu, L.-M. Sai, W.-Y. Lai, Q.-L. Fan, L.-H. Wang, W. Huang, *J. Phys. Chem. B* **2006**, *110*, 13370–13374.
[19] Y. He, L.-M. Sai, H.-T. Lu, M. Hu, W.-Y. Lai, Q.-L. Fan, L.-H. Wang, W. Huang, *Chem. Mater.* **2007**, *19*, 359–365.
[20] W. H. Suh, Y.-H. Suh, G. D. Stucky, *Nano Today* **2009**, *4*, 27–36.
[21] C. Chouly, L. Bordenave, R. Bareille, V. Guerin, A. Baquey, D. Pouliquen, C. Baquey, P. Jallet, *Clin. Mater.* **1994**, *15*, 293–301.
[22] C. M. Goodman, C. D. McCusker, T. Yilmaz, V. M. Rotello, *Bioconjugate Chem.* **2004**, *15*, 897–900.
[23] F. Y. Cheng, C. H. Su, Y. S. Yang, C. S. Yeh, C. Y. Tsai, C. L. Wu, M. T. Wu, D. B. Shieh, *Biomaterials* **2005**, *26*, 729–738.
[24] M. A. Dobrovolskaia, J. D. Clogston, B. W. Neun, J. B. Hall, A. K. Patri, S. E. McNeil, *Nano Lett.* **2008**, *8*, 2180–2187.
[25] T. A. Ostomel, Q. Shi, P. K. Stoimenov, G. D. Stucky, *Langmuir* **2007**, *23*, 11233–11238.
[26] K. Stalder, W. Stober, *Nature* **1965**, *207*, 874–875.
[27] W. W. Yu, L. H. Qu, W. Z. Guo, X. G. Peng, *Chem. Mater.* **2003**, *15*, 2854–2860.
[28] R. K. Kainthan, M. Gnanamani, M. Ganguli, T. Ghosh, D. E. Brooks, S. Maiti, J. N. Kizhakkedathu, *Biomaterials* **2006**, *27*, 5377–5390.
[29] H. T. Uyeda, I. L. Medintz, J. K. Jaiswal, S. M. Simon, H. Mattoussi, *J. Am. Chem. Soc.* **2005**, *127*, 3870–3878.
[30] S. Roux, B. Garcia, J.-L. Bridot, M. Salomé, C. Marquette, L. Lemelle, P. Gillet, L. Blum, P. Perriat, O. Tillement, *Langmuir* **2005**, *21*, 2526–2536.
[31] D.-W. Deng, Y.-B. Qin, X. Yang, J.-S. Yu, Y. Pan, *J. Cryst. Growth* **2006**, *296*, 141–149.
[32] Y.-F. Liu, J.-S. Yu, *J. Colloid Interface Sci.* **2009**, *333*, 690–698.
[33] X. Gu, Y. Zheng, Y. Cheng, S. Zhong, T. Xi, *Biomaterials* **2009**, *30*, 484–498.
[34] M. Grabolle, M. Spieles, V. Lesnyak, N. Gaponik, A. Eychmüller, U. Resch-Genger, *Anal. Chem.* **2009**, *81*, 6285–6294.
[35] D. V. Talapin, A. L. Rogach, E. V. Shevchenko, A. Kornowski, M. Haase, H. Weller, *J. Am. Chem. Soc.* **2002**, *124*, 5782–5790.

Received: October 3, 2009
Published Online: February 19, 2010

